The Astrophysical Journal, 835:274 (7pp), 2017 February 1 doi:10.3847/1538-4357/835/2/274

Optical and Near-infrared Study of Nova V2676 Oph 2012

A. Raj[1,2], R. K. Das[3], and F. M. Walter[4]
[1] Korea Astronomy and Space Science Institute, Daejeon, 34055, Korea; ashish.raj@iiap.res.in
[2] Indian Institute of Astrophysics, II Block Koramangala, Bangalore 560 034, India
[3] Department of Astrophysics & Cosmology, S N Bose National Centre for Basic Sciences, Salt Lake, Kolkata 700106, India
[4] Department of Physics and Astronomy, Stony Brook University, Stony Brook, NY 11794-3800, USA
Received 2016 April 2; revised 2016 December 22; accepted 2016 December 22; published 2017 February 1

Abstract

We present optical spectrophotometric and near-infrared (NIR) photometric observations of the nova V2676 Oph covering the period from 2012 March 29 through 2015 May 8. The optical spectra and photometry of the nova have been taken from SMARTS and Asiago; the NIR photometry was obtained from SMARTS and Mt. Abu. The spectra were dominated by strong H I lines from the Balmer series, Fe II, N I, and [O I] lines in the initial days, typical of an Fe II type nova. The measured FWHM for the Hβ and Hα lines was 800–1200 km s^{-1}. There was pronounced dust formation starting 90 days after the outburst. The $J - K$ color was the largest among recent dust-forming novae.

Key words: infrared: stars – line: identification – novae, cataclysmic variables – stars: individual (V2676 Oph) – techniques: spectroscopic

Supporting material: machine-readable tables

1. Introduction

The classical novae are interacting binary star systems containing a Roche-lobe filling secondary, on or near the main sequence, which is losing hydrogen-rich material through the inner Lagrangian point to the degenerate white dwarf primary. The mass transfer results in the formation of an accretion disc around the white dwarf. Runway thermonuclear reactions on the white dwarf surface give rise to the thermonuclear outburst, the sudden brightening seen in these systems.

Nova V2676 Oph (Nova Oph 2012) was discovered on 2012 March 25.789 UT (which we define as $t = 0$) by Hideo Nishimura on three 13 s unfiltered CCD frames with limiting magnitude 13.5 at $V = 12.1$ (Nishimura et al. 2012). A low-resolution optical spectrum obtained on March 27.74 UT with the 1.3 m Araki telescope at Koyama Astronomical Observatory (Arai & Isogai 2012) showed Hα, Hβ, and O I lines having prominent P-Cygni profiles. The FWHM of the emission component of Hα was about 600 km s^{-1}, suggesting that the object is an Fe II-type classical nova. Another low-resolution spectrum taken by Imamura (2012) at a similar time on March 27.836 UT showed prominent emission lines of Hα, Hβ and Fe II which confirmed that the nova was of Fe II class.

The near-infrared (NIR) observations taken between March 28 and 30 UT also showed that the spectra are typically of a Fe II class nova having prominent H I emission lines of Paβ, Paγ and Brγ, Fe II and other Brackett-series lines (Rudy et al. 2012a). The other prominent features seen were C I, O I, N I and the Ca II IR triplet. Rudy et al. (2012b) reported the fundamental, first and second overtone bands of CO in emission on 2012 May 1 and 2 and suggested the strong possibility of dust formation in the nova ejecta.

In this paper we present optical and NIR observations of V2676 Oph. The outline of the paper is as follows: Section 2 describes the observations and data analysis techniques. The results obtained from these observations are discussed in Section 3 and the summary is given in Section 4.

2. Observations

2.1. Near-infrared Observations

Near-infrared observations were obtained using the 1.2 m telescope of Mt.Abu Infrared Observatory from 2012 March 29 to June 17 and the SMARTS/CTIO 1.3 m telescope with the Andicam dual channel photometer (see Walter et al. 2012 for a description of the of the instrument and the data reductions). The log of the photometric observations from Mt. Abu is given in Table 1 and the SMARTS photometry is available on the SMARTS atlas. Photometry in the *JHK* bands was done under clear sky conditions using a NIR Imager/Spectrometer with a 256 × 256 HgCdTe NICMOS3 array in the imaging mode. Several frames, at four dithered positions, offset by ∼30 arcsec were obtained in all the bands. The sky frames, which are subtracted from the nova frames, were generated by median-combining the dithered frames (see Raj et al. 2013 for more details). The standard star SAO 185406 (spectral type—B9.5/A0V) having *JHK* magnitudes 6.47, 6.53, and 6.53 respectively, was used for photometric calibration. The data were reduced and analyzed using the IRAF package.

2.2. Optical Observations

Optical spectra were obtained with the Asiago 1.22 m telescope + B&C spectrograph, 2 arcsec slit width and oriented along north–south. The calibration in absolute fluxes for each nova spectrum was done by observations of several spectrophotometric standards observed on the same night around similar airmasses. A more detailed description of Asiago Novae and Symbiotic stars (ANS) Collaboration instruments, operation modes, and results on the monitoring of novae can be found in Munari et al. (2012).

Further low-dispersion spectra and photometry were obtained using the SMARTS facilities.[5] The R-C grating

[5] http://www.astro.sunysb.edu/fwalter/SMARTS/NovaAtlas.

spectrograph, the data reduction techniques, and the observing modes are described by Walter et al. (2012). Basically, mode 13/*I* is sensitive to the entire optical band, from 3200 Å through 9500 Å; mode 26/Ia is sensitive from 3650 Å through 5400 Å; mode 47/*I* covers 5650 through 6900 Å; mode 47/IIb covers 4060 Å through 4720 Å. We obtained 19 spectra on an irregular cadence and with various sky conditions from 2012 April 5 through 2012 June 24. The target was observed using the COSMOS[6] long slit spectrograph at CTIO on 2015 May 8, some three years after the outburst. We used the r2k disperser in combination with the 3pxR slit and the OG570 filter to obtain wavelength coverage from 6082 Å through 10253 Å, with a reciprocal dispersion of 1 Å/pixel, and a resolution of about 3 Å. Data reductions are similar to those used for the SMARTS spectra. The log of the spectroscopic observations is given in Table 2.

Table 1
Log of the *JHK* Photometric Observations of Nova V2676 Oph from Mt. Abu

Date of observation 2012 (UT)	Days after discovery	Magnitudes		
		J	*H*	*K*
Mar 30	04	9.89 ± 0.05	9.50 ± 0.06	9.41 ± 0.15
Apr 01	06	9.95 ± 0.04	9.46 ± 0.12	9.17 ± 0.15
Apr 03	08	9.29 ± 0.04	8.97 ± 0.09	8.61 ± 0.16
Apr 04	09	8.94 ± 0.04	8.49 ± 0.09	8.14 ± 0.10
May 27	62	8.93 ± 0.07	8.49 ± 0.09	7.69 ± 0.07
May 28	63	8.89 ± 0.07	8.38 ± 0.03	7.53 ± 0.21
May 29	64	8.86 ± 0.03	8.46 ± 0.03	8.29 ± 0.09
May 30	65	8.89 ± 0.04	8.39 ± 0.01	7.82 ± 0.12
May 31	66	9.18 ± 0.08	8.70 ± 0.05	8.28 ± 0.09
Jun 01	67	8.67 ± 0.04	8.28 ± 0.03	7.88 ± 0.12
Jun 02	68	9.10 ± 0.04	8.75 ± 0.13	8.59 ± 0.03
Jun 03	69	8.73 ± 0.04	8.40 ± 0.07	8.42 ± 0.03
Jun 07	73	8.61 ± 0.05	8.29 ± 0.03	8.30 ± 0.20
Jun 09	75	8.81 ± 0.01	8.29 ± 0.03	7.35 ± 0.19
Jun 18	84	9.39 ± 0.06	8.53 ± 0.02	7.27 ± 0.13

3. Results

3.1. General Characteristics of V and JHK Band Light Curves

The *V* and *JHK* band light curves are made using the data from the American Association of Variable Star Observers (AAVSO), SMARTS/CTIO 1.3 m (Walter et al. 2012), Asiago 1.22 m and Mt. Abu 1.2 m telescope facilities (see Figure 1). The *V* band light curve shows fluctuations of ∼0.7 magnitude around $m_v = 11.5$ up to 70 days from outburst before beginning a slow decline. A sudden drop of more than 5 mag commencing after 90 days clearly indicates the dust formation in the nova ejecta (see Figure 1, lower panel). The nova faded to >23 mag between 110 and 210 days from the outburst, suggesting that a large amount of dust was formed in the nova ejecta. After day 215 it recovered to $V \sim 18$. Since day 400 it has faded slowly, to *B, V, R, I* magnitudes of about 21, 18.7, 18.3, and 19.2, respectively, in 2016 February.

The NIR *JHK* light curves are made using data from the Mt. Abu observations (see Table 1) and the SMARTS/CTIO 1.3 m telescope facility (Walter et al. 2012). The NIR light curves are complex. The initial trends are downward in *J* and more or less flat in *H* and *K*, with superposed fluctuations similar to those seen in the optical (see Figure 1). After about day 70 the *K*

Table 2
Log of the Spectroscopic Observations of Nova V2676 Oph from the Asiago 1.22 m and SMARTS 1.5 m Telescopes

Date of Observation (UT)	Days after Discovery	Time (s)	Mode	Resolution	Observatory or Instrument
(2012)					
Apr 04	10	1500	13/I	17 Å	SMARTS
Apr 16	22	900	47/Ib	3.1 Å	SMARTS
Apr 20	26	900	13/I	17 Å	SMARTS
Apr 22	28	900	47/Ib	3.1 Å	SMARTS
Apr 28	34	900	26/Ia	4.4 Å	SMARTS
Apr 30	36	900	47/Ib	3.1 Å	SMARTS
May 04	40	900	47/Ib	3.1 Å	SMARTS
May 08	44	900	47/Ib	3.1 Å	SMARTS
May 09	45	900	26/Ia	4.4 Å	SMARTS
May 10	46	900	⋯	2.31 Å	ASIAGO
May 16	52	900	26/Ia	4.4 Å	SMARTS
May 17	53	1200	⋯	2.31 Å	ASIAGO
May 27	63	900	26/Ia	4.4 Å	SMARTS
May 28	64	1800	47/IIb	1.6 Å	SMARTS
May 29	65	900	26/Ia	4.4 Å	SMARTS
May 30	66	900	47/Ib	3.1 Å	SMARTS
May 31	67	900	26/Ia	4.4 Å	SMARTS
Jun 02	69	900	47/Ib	3.1 Å	SMARTS
Jun 16	83	1800	⋯	2.31 Å	ASIAGO
Jun 20	87	900	13/I	17 Å	SMARTS
Jun 22	89	900	47/Ib	3.1 Å	SMARTS
Jun 24	91	900	26/Ia	4.4 Å	SMARTS
(2015)					
May 08	1138	3600	⋯	3 Å	CTIO

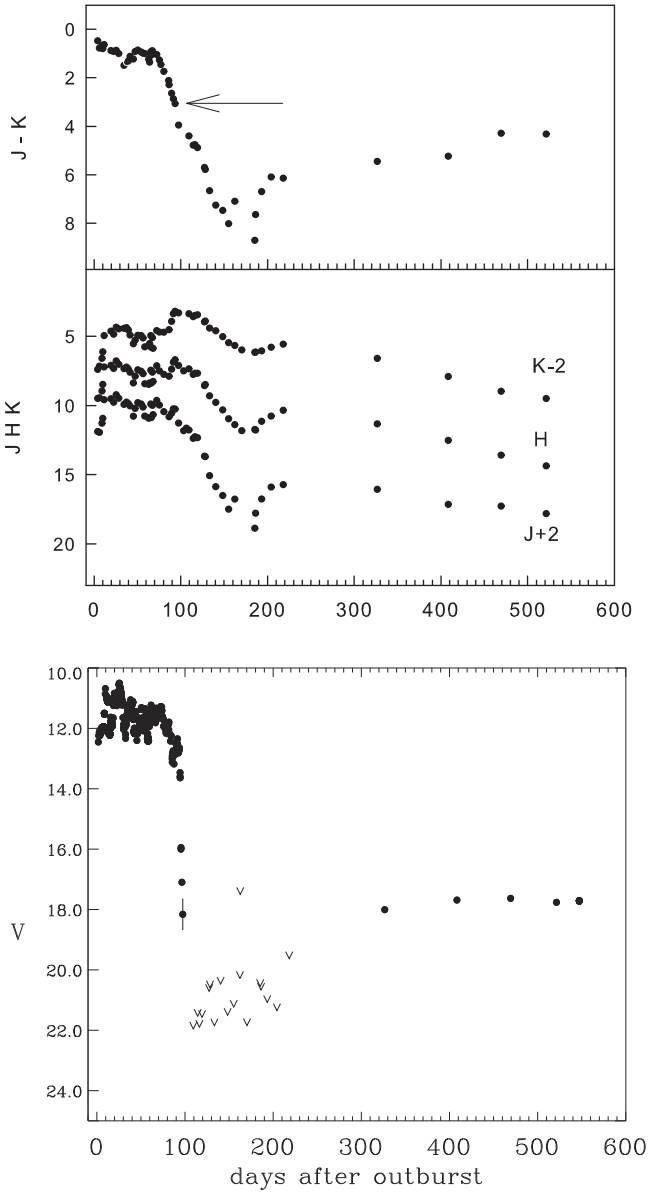

Figure 1. *V* and *JHK* band light curves of V2676 Oph based on the data obtained from the Mt. Abu, Asiago and SMARTS/CTIO facilities. The sudden fall in the *V* band light curve (lower panel) after 90 days from the outburst clearly indicates the onset of dust formation in the nova ejecta. Upper limits are 1σ.

band brightness increased by over 2 mag, accompanied by a smaller brightening in *H*, while *J* continued to fade.

The *K* band brightness reached a peak value of ∼5.2 on day 93; the $J-K$ and $H-K$ colors were about 3.1 (marked in Figure 1) and 1.5, respectively. These NIR color excesses indicate that dust has been formed in the nova ejecta. Thereafter, the *JHK* band light curves showed a steep, steady decline from 100 to 190 days from the outburst, lagging the dust dip seen in the optical. After day 190, the NIR brightness started recovering to brighter levels. The deep NIR dip suggests that the dust emission is optically thick even out to 2.2 μm. The dip is both shallower and narrower than the optical dip, consistent with dust opacity. After recovering, the NIR fluxes faded at a rate of about 0.015 mag day^{-1} until the target became too faint to follow with Andicam after 2014 August 14 (about day 700). At that time the $J-K$ color had decreased to about 3 mag, which is consistent with a 1500–2000 K blackbody dust shell. Varricatt et al. (2013) reported NIR photometry between 2012 September 6 and 2013 April 9 which confirms the presence of the dust shell.

3.2. The Reddening and Distance of V2676 Oph

From the optical spectra presented in this paper, we estimate the reddening $A_V = 2.9 \pm 0.1$ for the V2676 Oph using the Balmer decrement method assuming the electron density $\sim 10^6$ cm^{-3} and temperature ∼5000 K (see Section 3.5 for more details). However, it should be noted that the hydrogen-recombination lines are usually not described by the Case B approximation in novae and consequently the uncertainty in $E(B-V)$ from this method is likely to be underestimated. The value for A_V derived earlier is comparable with other estimated values for reddening e.g., $A_V = 2.39 \pm 0.12$ (Nagashima et al. 2015) and $A_V = 2.67 \pm 0.16$ (Kawakita et al. 2016) for $R = 3.1$ in the case of V2676 Oph. Alternatively, we can find the value of extinction from reddening $E(B-V) \sim 0.93$ toward the nova direction taken from Schlafly & Finkbeiner (2011) which was estimated using the colors of stars with spectra in the Sloan Digital Sky Survey. This gives an interstellar extinction $A_V \sim 2.89$ for $R = 3.1$ toward the nova direction. Though the value of A_V derived from our spectra is close to the Schlafly & Finkbeiner (2011) value, the values for electron density and temperature are specific for the region where [O I] forms and are unlikely to be applicable to the region containing the H. Hence, we use the value derived by Schlafly & Finkbeiner (2011) for reddening.

Since the brightness of the nova does not decline smoothly and there is large drop in magnitude due to dust formation, it is difficult to measure the characteristic time t_2, the time to decline by two magnitudes from visual maximum of the nova directly from the light curve. Instead, we can use the relation given by Williams et al. (2013) to show that, given that the dust starts to condense about day 90, t_2 is likely to be between 60 and 80 days. This indicates that V2676 Oph is a moderately fast nova.

Applying the maximum magnitude rate of decline (MMRD) relation by Downess & Duerbeck (2000) and the extinction value as mentioned above, we estimate the range for $M_{V_{\max}}$ to be between −6.5 and −6.8. Using this range for $M_{V_{\max}}$ together with the value of the visual maximum $V_{\max} = 10.6$ on April 5, we estimate the range for the distance d to the nova to be between 6.9 and 7.9 kpc and the height z of the nova to be in the range 637–730 pc above the Galactic plane. The large reddening is consistent with the location near the Galactic center (l, $b = 0.26, +5.30$) and the large distance.

3.3. Line Identification, Evolution, and General Characteristics of the Optical Spectra

The optical spectra from SMARTS and Asiago, presented in Figure 2, cover the pre-maximum to the early decline phase with one spectrum in the nebular phase. We obtained 19 low-dispersion spectra using the SMARTS 1.5 m/RC spectrograph from 2012 April 5 through 2012 June 24 (days 11 through 91). The initial spectrum covered the entire available spectrum at low dispersion. Hα was in emission

[6] http://www.ctio.noao.edu/noao/content/cosmos.

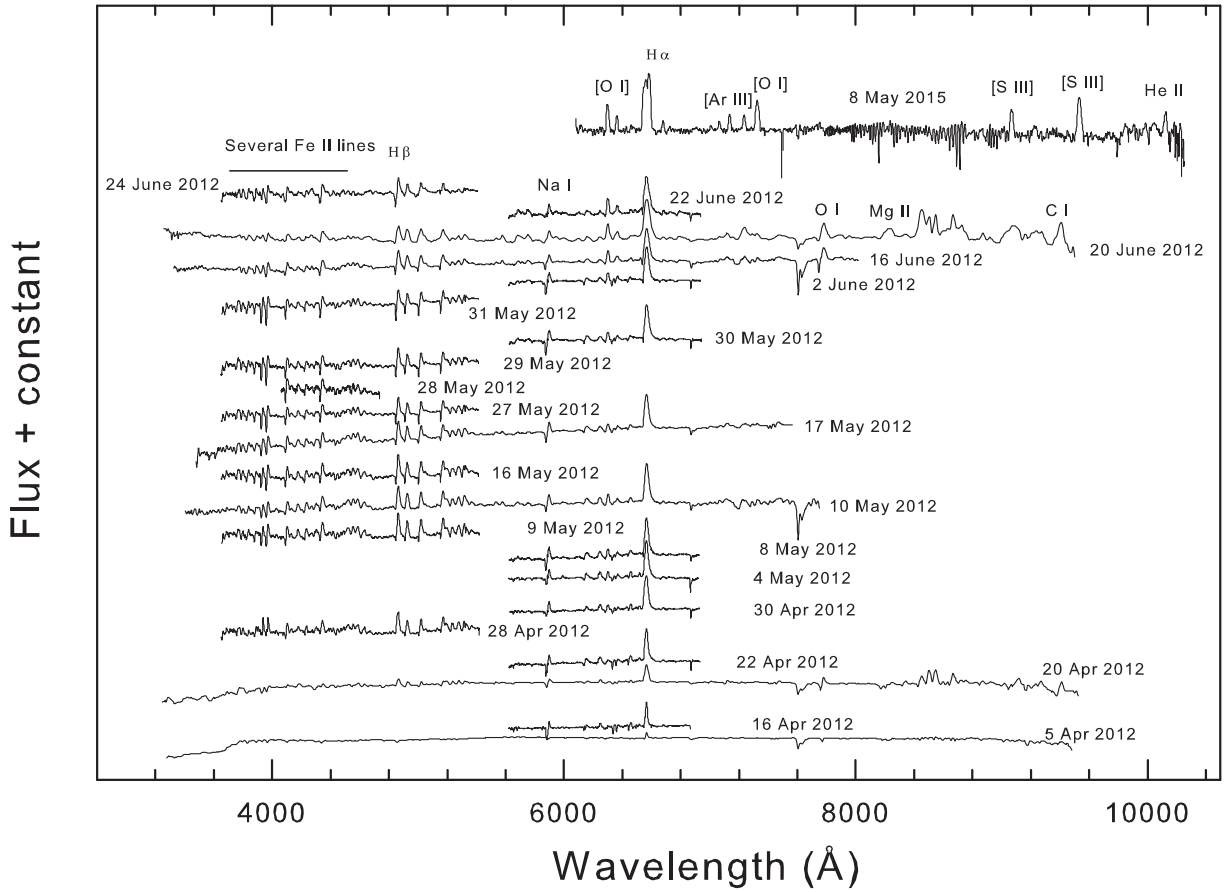

Figure 2. Low-resolution optical spectra of V2676 Oph presented at different epochs to show the spectroscopic evolution from pre-maximum to post-maximum phase. These observations have been taken from SMARTS and Asiago.

(EW ~ -7.3Å), with a P-Cygni absorption evident (EW $\sim$ 0.6 Å). No other lines are seen in emission. The H I Balmer series is seen in absorption at least through H-10, and Paschen lines Pa9–Pa12 also seem to be present. At this low dispersion absorption lines can be hard to identify unambiguously, but other strong absorption lines include Ca II K and H, Na I (5890/5896; 6154/6160, 8191), possible O I 7774, and numerous lines that may be Fe II multiplets 27, 28, 37, 38, and 74. By day 22 the strength of the Hα emission had grown to an EW of -63 Å. At 3.1 Å resolution the line is asymmetric, with a notch about 350 km s^{-1} blueward of the emission peak. Na I D is in emission with a strong P-Cygni absorption feature. The Na I 6154/6160 lines are in emission, with absorption components at -600 km s^{-1}. He I 6678 is in emission. The strong absorption may be P-Cygni outflows (and weak emission) in Si II 6347 and various Fe II multiplet 74 lines.

A low-resolution spectrum on day 26 shows many emission lines, including the Balmer lines through H-10, the Fe II multiplet 42, 48, 49, and 55 lines, and the Ca II infrared triplet. The equivalent width of Hα remained at -63 Å. Prominent P-Cygni lines are seen at Na I D and 6154/6160, O I 7002, 7774, 8446, C I 7120, N I 7450, Ca IIK and H are in absorption. On day 28 the Na I D1 and D2 absorption components are well-defined, at -660 km s^{-1}. The Hα equivalent width had increased to -165 Å; the line profile is asymmetric with a notch 320 km s^{-1} blueward of the peak and a red tail extending to about 1500 km s^{-1}. Our first blue spectrum, on day 34, shows a typical Fe II nova spectrum. Hβ is the strongest line, followed by Ca II-K and H and the Fe II multiplet 42 lines. The latter show narrow P-Cygni absorption at -950 km s^{-1}. By day 46 this narrow fast P-Cygni outflow was also visible in the Balmer lines (Hβ through H-11). This absorption component persisted at least through day 67, by which time it had accelerated to a velocity of about -1000 km s^{-1}. The first two Asiago spectra were obtained in the midst of these, on days 45 and 52. The strong outflow in the Na I D lines which had persisted through day 69 (EW $\sim$ 9 Å) weakened by about a factor of 10 by day 89. At this time, based on a P-Cygni line profile at He I 6678, there may be similar emission at He I 5876 complicating the line profile. Also by day 89, Hα and the 6300/6364 Å [O I] lines are developing double-horned line profiles, with $V > R$. The Hα equivalent width was -400 Å. In our last (blue) spectrum, on day 91, or about a week after the final Asiago spectrum, the P-Cygni absorption components (velocity ~ -1100 km s^{-1}) of the Balmer lines remain prominent, while those of the Fe II lines are less distinct. The re-appearance of P-Cygni profiles in the later phase have been seen in other novae e.g., V1186 Sco, V2540 Oph, V4745 Sgr, V5113 Sgr, V458 Vul, and V378 Ser (Tanaka et al. 2011). This can be attributed to a re-expansion of the photosphere (see Tanaka et al. 2011 for more details).

The COSMOS spectrum taken on 2015 May 8 shows that the nova was in the nebular phase. In the 6100–10200 Å spectral range the strongest line by far is Hα+[N II] 6548/6584, followed by the forbidden lines of [S III] 9531, the four [O II] lines from 7319 to 7331 Å, and [O I] 6300 and [Ar III]

Table 3
Reddening-corrected Fluxes (in erg s^{-1} cm^{-2}) for Prominent Emission Lines Corrected for $A_V = 2.89$

Wavelength (Å)	Species	Apr 28	May 10
3934	Ca II	1.37E−10	1.96E−11
3970	Ca II and Hϵ	1.49E−10	2.00E−11
4023	He I	1.57E−11	...
4101	Hδ	9.89E−11	2.08E−11
4129	Fe II(27)	2.52E−11	...
4173	Fe II(27)	3.06E−11	...
4178	Fe II(28)	...	1.45E−11
4233	Fe II(27)	4.73E−11	1.42E−11
4273	Fe II(27)	1.09E−11	5.24E−12
4303	Fe II(27)	3.35E−11	1.71E−11
4340	Hγ	1.21E−10	3.08E−11
4378	He I	6.52E−12	...
4488	N II	1.58E−11	...
4555	Fe II(37)	2.81E−11	8.50E−12
4586	Fe II(38)	5.42E−11	...
4634	N III	3.77E−11	9.64E−12
4861	Hβ	1.16E−10	5.59E−11
4924	Fe II(42)	7.96E−11	2.43E−11
5018	Fe II(42)	7.25E−11	2.32E−11
5169	Fe II + Mg I	6.03E−11	1.86E−11
5235	Fe II(49)	3.24E−11	7.83E−12
5276	Fe II(49+48)	4.46E−11	1.04E−11
5316	Fe II(49)	1.84E−11	1.48E−11
5361	Fe II(48)	...	3.97E−12
5528	Mg I	...	3.41E−12
5577	[O I]	...	4.10E−12
5676	N II	...	2.83E−12
5755	[N II](3)	...	2.53E−12
5890–5896	Na I	...	1.31E−11
5991	Fe II(46)	...	1.92E−12
6154–6160	Na I	...	7.31E−12
6243	Fe II + N II	...	7.63E−12
6300	[O I]	...	1.25E−11
6364	[O I]	...	3.58E−12
6419	Fe II(74)	...	1.04E−12
6456	Fe II	...	3.48E−12
6563	Hα	...	1.89E−10

(This table is available in its entirety in machine-readable form.)

Table 4
Reddening-corrected Fluxes (in erg s^{-1} cm^{-2}) for Prominent Emission Lines Corrected for $A_V = 2.89$

Wavelength (Å)	Species	May 17	Jun 16
3934	Ca II	4.66E−11	3.75E−11
3970	Ca II and Hϵ	4.81E−11	4.42E−11
4101	Hδ	3.55E−11	4.18E−11
4178	Fe II(28)	2.90E−11	1.50E−12
4233	Fe II(27)	2.28E−11	2.33E−11
4340	Hγ	4.89E−11	5.77E−11
4586	Fe II(38)	2.22E−11	1.39E−12
4634	N III	1.50E−11	1.26E−11
4861	Hβ	6.33E−11	5.19E−11
4924	Fe II(42)	5.00E−11	5.17E−11
5018	Fe II(42)	4.62E−11	4.81E−11
5169	Fe II + Mg I	8.27E−11	6.36E−11
5235	Fe II(49)	1.91E−11	7.38E−12
5276	Fe II(49+48)	2.35E−11	1.33E−12
5316	Fe II(49)	3.17E−11	1.94E−12
5577	[O I]	3.26E−12	3.74E−12
5890–5896	Na I	2.96E−11	1.99E−11
6154–6160	Na I	2.49E−11	1.25E−11
6243	Fe II + N II	2.02E−11	1.13E−11
6300	[O I]	1.65E−11	1.49E−11
6364	[O I]	7.53E−12	7.81E−12
6456	Fe II	1.15E−11	5.44E−12
6563	Hα	4.99E−11	3.56E−10
6678	He I	3.33E−12	3.36E−11
7120	C I	1.07E−11	5.29E−12
7237	[Ar IV]	1.79E−11	1.47E−11
7477	O I	1.73E−11	8.22E−12

(This table is available in its entirety in machine-readable form.)

7751. The only permitted lines are Hα and some He I and He II lines. Overall the spectrum resembles that of V443 Sct some two years after its outburst (Williams et al. 1994). The Hα +[N II] lines appear to be resolved, and can be fit as a sum of three Gaussians. The median FWHM is 623 km s^{-1}, while the instrumental resolution is about 100 km s^{-1}. Radial velocities are measured from the line centroids. The median radial velocity is 6 km s^{-1}, with uncertainties of order 50 km s^{-1}, from convolving measurement errors with uncertainties in line rest wavelengths. Our observations are consistent with the results of Nagashima et al. (2014, 2015) and Kawakita et al. (2015, 2016). A list of the prominent lines identified and the reddening-corrected emission line fluxes (in erg s^{-1} cm^{-2}) for selected epochs is given in Tables 3–5. The complete tables are available in the online version of the paper.

3.4. Dust Formation and $J - K$ Colors

A sharp decline in the optical light curve (the dust dip) about 90 days after the outburst and a steady increase in the NIR magnitudes, especially in the K band, clearly indicate the onset of the dust formation. The dust dip in the $BVRI$ band light curves is very similar to that in the nova V5668 Sgr which, like V2676 Oph, also shows the CO band in emission (Banerjee et al. 2016). The presence of CO molecules in early nova spectra are indicators of low-temperature zones which are conducive to dust formation in the nova ejecta. This is clearly confirmed in the case of V2676 Oph. However, only 10 novae have so far shown the CO bands in emission before the dust formation (Raj et al. 2015; Banerjee et al. 2016) and there are many cases such as V1280 Sco (see Das et al. 2008) and V5579 Sgr (Raj et al. 2011) where dust formation was reported without any CO emission. The reason is not clearly understood; possibly these molecules were present but the strengths were below detection levels or due to observational constraints they might have been formed and destroyed before the detection.

An increase in flux in the H and K bands coincides with the onset of the dust dip at shorter wavelengths. This is likely thermal emission from the dust. The larger excess in K is consistent with expectations that the thermal emission will peak in or beyond the K band. Similar behavior was seen in V5579 Sgr (Raj et al. 2011) and V496 Sct (Raj et al. 2012), which also showed dust formation. The $J - K$ color excess reached a maximum of ∼8 mag at 190 days from outburst. This seems to be the largest $J - K$ value observed for dust forming novae in recent years; $(J - K) = 2.76$ for V5579 Sgr (Raj et al. 2011), 3.79 for V496 Sct (Raj et al. 2012), 4.58 for V5584 Sgr (Raj et al. 2015), 4.65 for V1280 Sco (Das et al. 2008), and 3.97 for V2615 Oph (Das et al. 2009). There

Table 5
Reddening-corrected Fluxes (in erg s^{-1} cm^{-2}) for Prominent Emission Lines Corrected for $A_V = 2.89$

Wavelength (Å)	Species	Jun 20	2015 May 8
3934	Ca II	2.89E−11	⋯
3970	Ca II and Hϵ	3.43E−11	⋯
4101	Hδ	5.51E−12	⋯
4178	Fe II(28)	1.65E−12	⋯
4340	Hγ	7.84E−11	⋯
4555	Fe II(37)	6.46E−12	⋯
4663	Al II	2.94E−12	⋯
4861	Hβ	1.45E−11	⋯
4924	Fe II(42)	4.71E−11	⋯
5018	Fe II(42)	6.27E−12	⋯
5169	Fe II + Mg I	4.08E−12	⋯
5235	Fe II(49)	3.28E−12	⋯
5276	Fe II(49+48)	6.61E−12	⋯
5316	Fe II(49)	1.35E−11	⋯
5535	Fe II(55) + N II	2.66E−12	⋯
5577	[O I]	9.27E−12	⋯
5755	[N II](3)	1.13E−11	⋯
5890–5896	Na I	1.88E−11	⋯
5942	N II(28)	2.54E−12	⋯
6154–6160	Na I	9.73E−12	⋯
6243	Fe II + N II	4.80E−12	1.89E−13
6300	[O I]	3.69E−11	4.84E−12
6364	[O I]	1.54E−11	1.59E−12
6563	Hα	8.20E−11	1.76E−10
6678	He I	2.23E−12	8.24E−13
6716–6730	[S II]	2.64E−12	1.84E−13
7002	[O I]	⋯	2.23E−13
7065	He I	⋯	5.32E−13
7281	He I	⋯	9.04E−14
7319–7331	[O II]	⋯	5.65E−12
9069	[S III]	⋯	1.57E−12
9531	[S III]	⋯	4.21E−12
10126	He II	⋯	8.16E−13

(This table is available in its entirety in machine-readable form.)

after the $J - K$ color decreased, presumably because the dust thinned due to geometrical dilution.

The presence of strong C I lines and the early dust formation (just after 90 days) in the case of V2676 Oph indicate the presence of carbon grains in the dust shell (Clayton & Wickramasinghe 1976). This is further supported by the detection of C_2 and CN molecules in V2676 Oph in the early phase (Nagashima et al. 2014).

3.5. Physical Parameters

Optical spectra can be helpful for estimating the physical parameters of nova ejecta with the use of hydrogen and oxygen line fluxes. The electron number densities are large in the early phase of nova evolution, thus the optical depth τ, which is an important parameter, can be used to estimate the elemental abundances. Using the formulation of Williams (1994),

$$\frac{j_{6300}}{j_{6364}} = \frac{1 - e^{-\tau}}{1 - e^{-\tau/3}}$$

we estimate the optical depth τ for the [O I] 6300 Å line for the period between 2012 May 10 and June 16, in the range of 1.1–1.7. Using the value of τ we can estimate the electron temperature given by the relation:

$$T_e = \frac{11{,}200}{\log\ [43\tau/(1 - e^{-\tau}) \times F_{\lambda 6300}/F_{\lambda 5577}]}$$

.We find $T_e \sim 4400$ K, which is consistent with other novae (Ederoclite et al. 2006). To estimate the mass of the hydrogen, m(H), we use the following relation from Osterbrock & Ferland (2006), which relates the intensity of the Hβ line and the mass of the hydrogen in the emitting nebula having pure hydrogen as,

$$m(H)/M_\odot = d^2 \times 2.455 \times 10^{-2} \times I(H\beta)/\alpha_{\rm eff} N_e$$

where $\alpha_{\rm eff}$ is the effective recombination coefficient taken from Storey & Hummer (1995) and $I(H\beta)$ is the flux for the Hβ line. We have used two $I(H\beta)$ flux values: 6.33×10^{-11} and 5.19×10^{-11} erg cm^{-2} s^{-1} for 2012 May 17 and June 16, respectively. The [O I] 6300, 6364 and 5577 Å lines are used to set the range for the electron density (N_e), 10^6–10^7 cm^{-3}. We do not notice any significant change in T_e and N_e estimated above for both epochs. The mass of hydrogen m(H) is estimated as $(2.7 \times 10^{-7}$–$3.3 \times 10^{-6})\, d^2\, M_\odot$ where d is the distance to the nova.

4. Summary

We have presented optical spectrophotometry and NIR photometry of nova V2676 Oph which erupted in late March 2012. The optical spectra indicate that the nova belongs to the Fe II class. The reddening and distance to the nova are calculated. The nova shows a large amount of dust formation 90 days after the outburst. The physical parameters, optical depth, electron temperature, and mass of hydrogen are estimated for V2676 Oph.

The research work at the Physical Research Laboratory was funded by the Department of Space, Government of India. Access to SMARTS is made possible by generous support from the Provost of Stony Brook University, Dennis Assanis. Based in part on observations at Cerro Tololo Inter-American Observatory, National Optical Astronomy Observatory (NOAO Prop. 2015A-0261, PI F.M. Walter, plus SMARTS time), which is operated by the Association of Universities for Research in Astronomy (AURA) under a cooperative agreement with the National Science Foundation. We thank the referee, Professor A. Evans, for his helpful comments as well as Prof. G. C. Anupama (IIA), Dr. U. S. Kamath (IIA) and Dr. B. C. Lee (KASI) for useful discussions. We acknowledge the use of AAVSO (American Association of Variable Star Observers) optical photometric data and the spectrophotometric data which was privately communicated by the Asiago *ANS* (Asiago Novae and Symbiotic stars) Collaboration team.

References

Arai, A., & Isogai, M. 2012, CBET, 3072, 2
Banerjee, D. P. K., Srivastava, M. K., Ashok, N. M., & Venkataraman, V. 2016, MNRAS, 455L, 109
Clayton, D. D., & Wickramasinghe, N. C. 1976, Ap&SS, 42, 463
Das, R. K., Banerjee, D. P. K., & Ashok, N. M. 2009, MNRAS, 398, 375
Das, R. K., Banerjee, D. P. K., Ashok, N. M., & Chesneau, O. 2008, MNRAS, 391, 1874
Downess, R. A., & Duerbeck, H. W. 2000, AJ, 120, 2007
Ederoclite, A., Mason, E., Della Valle, M., et al. 2006, A&A, 459, 875

Imamura, K. 2012, CBET, 3072, 3
Kawakita, H., Arai, A., & Fujii, M. 2016, PASJ, 68, 87
Kawakita, H., Fujii, M., Nagashima, M., et al. 2015, PASJ, 67, 17
Munari, U., Bacci, S., Baldinelli, L., et al. 2012, BaltA, 21, 13
Nagashima, M., Arai, A., Kajikawa, T., et al. 2014, ApJL, 780, 26
Nagashima, M., Arai, A., Kajikawa, T., et al. 2015, AcPPP, 2, 212
Nishimura, H., Kaneda, H., Kojima, T., & Yusa, T. 2012, CBET, 3072, 1
Osterbrock, D. E., & Ferland, G. J. 2006, Astrophysics of Gaseous Nebulae and Active Galactic Nuclei (2nd ed.; Sausalito, CA: Univ. Science Books)
Raj, A., Ashok, N. M., & Banerjee, D. P. K. 2011, MNRAS, 415, 3455
Raj, A., Ashok, N. M., Banerjee, D. P. K., et al. 2012, MNRAS, 425, 2576
Raj, A., Banerjee, D. P. K., & Ashok, N. M. 2013, MNRAS, 433, 2657
Raj, A., Banerjee, D. P. K., Ashok, N. M., & Kim, S. C. 2015, RAA, 15, 993
Rudy, R. J., Russell, R. W., Kim, D. L., et al. 2012a, CBET, 3081, 1
Rudy, R. J., Russell, R. W., Sitko, M. L., et al. 2012b, CBET, 3103, 1
Schlafly, E., & Finkbeiner, D. P. 2011, ApJ, 737, 103
Storey, P. J., & Hummer, D. G. 1995, MNRAS, 272, 41
Tanaka, J., Nogami, D., Fujii, M., Ayani, K., & Kato, T. 2011, PASJ, 63, 159
Varricatt, W. P., Carroll, T., Ehle, J., Wold, T., et al. 2013, ATel, 5090
Walter, F. M., Battisti, A., Towers, S. E., Bond, H. E., & Stringfellow, G. S. 2012, PASP, 124, 1057
Williams, R. E. 1994, ApJ, 426, 279
Williams, R. E., Phillips, M. M., & Hamuy, M. 1994, ApJS, 90, 297
Williams, S. C., Bode, M. F., Darnley, M. J., et al. 2013, ApJL, 777, L32